JOC The Journal of Organic Chemistry

Article

pubs.acs.org/joc

Discovery and Characterization of NK13650s, Naturally Occurring p300-Selective Histone Acetyltransferase Inhibitors

Shigehiro Tohyama,*[,†] Arihiro Tomura,*[,‡] Noriko Ikeda,[†] Masaki Hatano,[†] Junko Odanaka,[‡] Yumiko Kubota,[†] Maya Umekita,[†] Masayuki Igarashi,[†] Ryuichi Sawa,[†] and Tomio Morino[‡]

[†]Institute of Microbial Chemistry, Tokyo, 3-14-23 Kamiosaki, Shinagawa-ku, Tokyo 141-0021, Japan

[‡]Pharmaceuticals Research Laboratories, Research & Development Group, Nippon Kayaku, 3-31-12 Shimo, Kita-ku, Tokyo 115-8588, Japan

Supporting Information

ABSTRACT: The histone acetyltransferase (HAT) activity of p300 is essential for androgen receptor (AR) function. Androgen-independent prostate cancer cells require AR-mediated transcriptional activation for their growth. These observations indicate that p300 HAT is a promising target to overcome such hormone-resistant cancer cells. We sought p300 HAT inhibitors among microbial metabolites. By culturing a production strain belonging to *Penicillium*, we identified two new compounds, NK13650A and NK13650B, which were obtained as specific p300 HAT inhibitors. Structural analyses of these compounds elucidated that NK13650s have novel chemical structures comprising several amino acids and citrate. We applied a newly developed biosynthesis-based method to reveal the absolute configuration at the citrate quaternary carbon. This was accomplished by feeding a ^{13}C-labeled biosynthetic precursor of citrate. NK13650s selectively inhibited the activity of p300 HAT but not that of Tip60 HAT. NK13650s showed inhibitory activity against agonist-induced AR transcriptional activation, and NK13650A treatment inhibited hormone-dependent and -independent growth of prostate cancer cells.

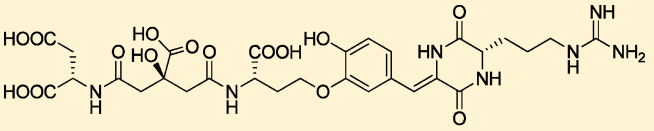

NK13650 A

INTRODUCTION

Histone acetyltransferases (HATs) acetylate not only histone but also many non-histone proteins that play important roles in apoptosis, inflammation, and the cell cycle.[1] One of these proteins is the androgen receptor (AR). Androgens are hormones related to the development and the function of male internal genitalia. They are also known as proliferation signals and the main cause of the promotion of prostate cancer.[2] Therefore, endocrine therapies that suppress androgen function are administered against such a cancer. For example, antiandrogens (e.g., flutamide and casodex) act antagonistically to androgens by combining with AR; LHRH agonists (e.g., leuplin and zoladex) suppress androgen production; and C17,20-lyase inhibitors (e.g., abiraterone acetate) have been developed as curative treatments for prostate cancer.[3,4] However, repetitive use of such treatments results in hormone-resistant cancer that is no longer dependent on androgens and shows resistance against such androgen ablation drugs. Therefore, development of a new curative treatment involving mechanisms other than control of androgen action is desired to overcome hormone refractory prostate cancer (HRPC).[5]

AR function is modulated by post-translational modifications such as acetylation, phosphorylation, ubiquitylation, and SUMOylation.[6−8] Several HATs, including p300, pCAF, and Tip60, are responsible for post-translational acetylation of AR and regulate its function.[9−11] AR-mediated transcriptional activation requires the acetylation to be catalyzed by p300 HAT, which acetylates AR at the C-terminal regions K630, K632, and K633 presented in the DNA binding site.[12] The mutants, which have acetylation mimics at these lysine residues, have been identified in prostate cancer cells and show resistance against antiandrogens.[13] Interleukin-6 (IL-6) is another AR-mediated proliferation signal that activates AR via a different pathway from androgens. It participates widely in HRPC progression. Regulation of p300 gene expression using siRNAs inhibited IL-6-mediated AR activation.[14−16] These data strongly suggest that inhibiting p300 HAT activity could control the growth of HRPC cells and that p300-mediated AR acetylation has great potential as a target for drug development.

HATs also control the level of histone acetylation with histone deacetylases (HDACs) and widely regulate transcription. Several reports mentioned that altering the balance of HAT and HDAC activities could lead to several diseases, such as cancers and neurodegenerative disorders.[1,17−19] HDACs have received attention as targets for anticancer drugs, and several of their inhibitors have been approved by FDA for the treatment of human cutaneous T-cell lymphoma.[20,21] Compared with studies of HDAC inhibitors, few studies focused on HATs. In the 2000s, because of energetic research by Kundu et al. to discover HAT inhibitors from plants, several known plant components were found to have HAT inhibitory activity. These bioactive plant-derived products included garcinol,[22] anacardic acid,[23] curcumin,[24] and plumbagin.[25] Moreover, cinnamoy,[1,26] isothiazolone,[27] and some

Received: July 25, 2012
Published: September 17, 2012

dx.doi.org/10.1021/jo301534b | J. Org. Chem. 2012, 77, 9044−9052

lysine-coenzyme A (Lys-CoA) derivatives are inhibitors chemically synthesized by different groups.[28−30] Nevertheless, none of these inhibitors showed p300 HAT selectivity and appropriate properties for drug development. A novel HAT inhibitor having a unique chemical structure and outstanding activity is desired. In the present study, we sought such HAT inhibitors from microorganisms. Many secondary metabolites produced by microbes have been developed as drugs, and microorganisms are believed to be capable of producing many more uncharacterized compounds. Therefore, culture broths of such microorganisms are recognized as attractive sources of novel compounds having a unique structure or bioactivity.

In the present study, we screened a microorganism broth library in our laboratory to find p300 HAT inhibitors and identified two novel compounds: NK13650A and NK13650B (Figure 1). These compounds were obtained as secondary

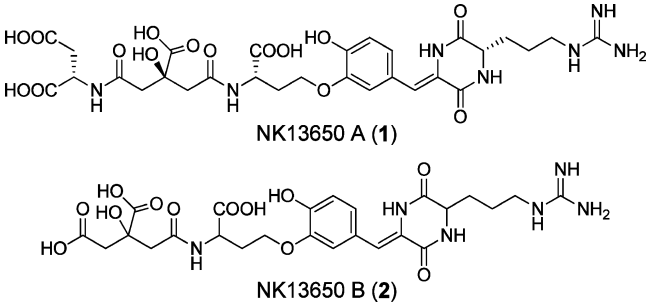

Figure 1. Structures of NK13650s.

metabolites of a *Penicillium* sp. NF13650 and showed strict selectivity for p300 HAT. Structural analyses demonstrated that these compounds have unique chemical structures; they are pseudopeptides containing citric acid. The citric acid had different substituents at C-1 and C-5 carboxyl groups, and the C-3 quaternary carbon accordingly became a chiral center. To elucidate this absolute configuration, we developed a useful biosynthesis-based method that involves feeding of a ^{13}C-labeled biosynthetic precursor of citrate. After investigating the bioactivities of these NK13650s, we revealed that they selectively inhibited p300 HAT activity and showed inhibitory activity against HRPC cells.

RESULTS

Screening and Discovery of NK13650s. The screening system to find new p300 HAT inhibitors was based on the method developed by Dr. Wynne Aherne.[31] Our libraries consisting of 19,320 culture broths of microbes were screened for p300 HAT inhibition. Four samples were regarded as "hits" (>50% inhibition of HAT activity). Two hit samples contained the same metabolite. However, we could not identify the active compound because of its low productivity or instability. 2-Methylfervenulone[32] was confirmed as an active substance in the third hit sample, but the sample did not show p300 HAT specificity. The last broth, produced by culturing the fungus *Penicillium* sp. NF13650, was expected to involve new components on the basis of preliminary tests. It was purified by two-step column chromatography and subsequent reverse phase HPLC. Consequently, two new compounds, NK13650A (**1**) as a major product and its minor derivative NK13650B (**2**), exhibiting obvious p300 HAT inhibitory activity were successfully isolated.

Planar Structure of NK13650s. The molecular formula of NK13650A was established as $C_{29}H_{37}N_7O_{15}$ on the basis of high-resolution electrospray ionization Fourier transform mass spectrometry (HRESIFT-MS). The ^{13}C NMR spectrum showed 29 signals: 8 of methylene, 8 methine, and 13 quaternary carbons by DEPT experiments (Table 1). NK13650A showed strong UV absorptions at 309 and 325 nm, and several assumedly aromatic signals (δ_C 110−150) were assigned in ^{13}C NMR, which indicated that NK13650A has an aromatic structure. The presence of multiple carbonyl groups was revealed by several carbon signals (δ_C 150−170) and sharp IR absorbance at 1720, 1668, and 1635 cm^{-1}, and methine carbons (δ_C 48.6, 49.5, and 54.7) expected to be derived from the α-position of amino acids were confirmed. These observations suggested that NK13650A was a type of peptide compound.

Two-dimensional NMR techniques (COSY, HMQC, and HMBC) were used to elucidate the five components of NK13650A (Figure 2). ^1H COSY correlations from *arg*-NH to *arg*6-NH as well as HMBC correlations from *arg*2-CH to *arg*1-amide carbon (δ_C 166.9) and *arg*5-CH_2 to *arg*7-guanidine carbon (δ_C 156.8) revealed the presence of arginine. The aspartate residue was determined by $^1H-^1H$ COSY correlations of *asp*-NH thru *asp*3-CH_2 as well as HMBC correlations from *asp*-NH and *asp*3-CH_2 to *asp*1-carboxylic acid (δ_C 172.4) and *asp*4-carboxylic acid (δ_C 171.8), respectively. COSY correlations from *hse*-NH to *hse*4-oxy methylene and an HMBC correlation from *hse*2-CH to *hse*1-carboxylic acid carbon (δ_C 173.4) revealed a 4-substituted-homoserine structure. The $^1H-^1H$ spin coupling network within an olefinic proton (δ_H 6.62) and three aromatic protons (δ_H 6.81, 7.01, and 7.01) and the HMBC coupling pattern from these protons and *dhdopa*-NH (Figure 2) revealed a dehydro-dihydroxyphenylalanine (DOPA). The geometry of dehydro-DOPA was determined as a *cis*-position because of the observation of ROE between *dhdopa*-NH and *dhdopa*5,9-*o*-benzene protons. The citrate residue was confirmed based on HMBC correlations of *cit*2- and *cit*4-methylene protons to *cit*3-quaternary carbon (δ_C 73.5) and *cit*3′-carboxylic acid (δ_C 174.8) was observed to be in parallel. On the basis of these results, all ^{13}C NMR signals were assigned appropriately. NK13650A was revealed to be a peptide-like compound comprising five components: arginine, aspartate, homoserine, dehydro-DOPA, and citrate.

Connections between these components were further established by HMBC spectroscopy. Observations of long-range coupling from *asp*2-CH to *cit*1-carbonyl carbon and *hse*2-CH to *cit*5-carbonyl carbon clarified that aspartate and homoserine residues were linked to *cit*1- and *cit*5-carbonyl as amide bonds. HMBC correlation from *hse*4-CH_2 to *dhdopa*6-quaternary aromatic carbon (δ_C 146.6) elucidated the presence of an ether bond between the *hse*4- and *dhdopa*6-position. HMBC coupling from *arg*-NH to *dhdopa*1-carbonyl and *dhdopa*2-C was confirmed, and correlation from *dhdopa*-NH to *arg*1-carbonyl and *arg*2-CH was present. Therefore, the formation of a diketopiperazine ring between arginine and dehydro-DOPA was definitely identified. Hence, the five components comprising NK13650A were linearly connected in the order aspartate, citrate, homoserine, dehydro-DOPA, and arginine through two amide bonds, an ether bond, and a diketopiperazine ring. The planar structure of NK13650A was determined (Figure 2).

NK13650B obtained as a minor product showed UV and IR spectra very similar to those of NK13650A. Therefore, it was

dx.doi.org/10.1021/jo301534b | J. Org. Chem. 2012, 77, 9044−9052

Table 1. ^{1}H (600 MHz) and ^{13}C (150 MHz) NMR Spectral Assignment of NK13650s in 0.5% TFA/DMSO-d_6

			NK13650A				NK13650B			
position		type	δ_C		δ_H	J (Hz)	δ_C		δ_H	J (Hz)
arg	1	C=O	166.9	s			166.9	s		
	2	CH	54.7	d	4.01	m, 1H	54.7	d	4.01	m, 1H
	3	CH_2	31.3	t	1.72	dt, 9.9, 6.1, 2H	31.3	t	1.72	dt, 10.0, 5.8, 2H
	4	CH_2	24.2	t	1.53	m, 2H	24.2	t	1.53	m, 2H
	5	CH_2	40.5	t	3.11	q, 6.6, 1H	40.5	t	3.10	q, 6.5, 1H
	6	NH			7.48	brt, 5.7, 1H			7.48	t, 6.0, 1H
	7	C=N	156.8	s			156.8	s		
		NH			8.39	d, 2.7, 1H			5.03	d, 2.4, 1H
dhdopa	1	C=O	160.9	s			160.9	s		
	2	C	124.6	s			124.6	s		
	3	CH	115.5	d	6.62	s, 1H	115.5	d	6.62	s, 1H
	4	C	124.7	s			124.7	s		
	5	CH	115.7	d	7.01	d,1.7, 1H	115.7	d	7.01	d, 1.7, 1H
	6	C	146.6	s			146.6	s		
	7	C	147.6	s			147.6	s		
	8	CH	116.0	d	6.81	d, 8.2, 1H	116.0	d	6.81	d, 8.0, 1H
	9	CH	123.1	d	7.01	dd, 1.7, 8.2, 1H	123.1	d	6.99	dd, 1.7, 8.0, 1H
		NH			9.81	s, 1H			9.80	s, 1H
hse	1	CO_2H	173.4	s			173.4	s		
	2	CH	49.5	d	4.41	dt, 4.8, 8.5, 1H	49.5	d	4.42	ddd, 8.9, 7.2, 5.2, 1H
	3	CH_2	30.9	t	2.00	ddt, 8.6, 14.4, 5.8, 1H	30.9	t	2.00	ddt, 8.9, 14.1, 5.8, 1H
					2.18	br-dq, 12.4, 6.5, 1H			2.19	dq, 6.5, 14.1, 1H
	4	CH_2	65.5	t	3.94−4.07	m, 2H	65.5	t	4.00	m, 1H
									4.05	dt, 10.9, 5.9, 1H
		NH			8.26	d, 4.7, 1H			8.27	d, 7.7, 1H
citrate	1	C=O	169.5	s			171.5	s		
	2	CH_2	43.2	t	2.55−2.67	m, 2H	43.1	t	2.62	d, 15.6, 1H
									2.74	d, 15.6, 1H
	3	C	73.5	s			73.0	s		
	4	CH_2	43.2	t	2.55−2.67	m, 2H	43.3	t	2.55−2.67	d, 14.8, 1H
										d, 14.8, 1H
	5	C=O	169.7	s			169.7	s		
	3′	CO_2H	174.9	s			174.8	s		
asp	1	CO_2H	172.4	s						
	2	CH	48.6	d	4.51	dt, 7.9, 6.2, 1H				
	3	CH_2	36.3	t	2.53−2.67	m, 2H				
	4	CO_2H	171.8	s						
		NH			8.26	d, 7.9, 1H				

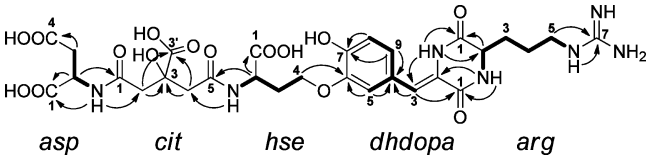

Figure 2. Structure determination of NK13650A by two-dimensional NMR techniques. COSY correlations are shown as bold bonds, and key HMBC long-range couplings are indicated by arrows.

considered that NK13650B was related to NK13650A. In ^{1}H and ^{13}C NMR spectra, NK13650B was similar to NK13650A, except for the lack of an aspartate moiety (Table 1). HR ESIFT-MS analyses established the molecular formula of NK13650B as $C_{25}H_{32}N_6O_{12}$. Indeed, an effort to elucidate the framework of NK13650B (Supporting Information) revealed that it had the expected structure shown in Figure 1.

Absolute Configurations of Amino Acids Involved in NK13650A. Absolute configurations of each amino acid were determined by an advanced version of Marfey's method.[33,34] The hydrolysate (prepared by treating NK13650A with HCl under heat) was derivatized with 1-fluoro-2,4-dinitrophenyl-5-L-leucineamide (L-FDLA), and in parallel, authentic derivatives were prepared with L-FDLA and both stereoisomers of the amino acids aspartate, arginine, and homoserine. The resulting samples were analyzed by HPLC-HRESI-FTMS and by high-resolution extracted ion chromatograph of each protonated molecule (m/z 428.1418 for aspartic acid; 469.2159 for arginine; and 414.1625 for homoserine, m/z tolerance 0.004) (Figure 3). The 2,4-dinitrophenyl-5-L-leucineamide (L-DLA) derivative of aspartate originating from the hydrolysate showed the same peak as the L-aspartate derivative (Figure 3A), clearly indicating that the aspartate moiety in NK13650A had a L-configuration. Similarly, arginine and homoserine were determined to have an L-conformation (Figure 3B and C). All chiral centers originating from the amino acids in NK13650A were confirmed to have an *S* configuration.

Absolute Configuration at the Center Carbon in Citrate. An absolute configuration of the quaternary carbon in citrate at *cit*3 remained unclear. Because the chiral center is

dx.doi.org/10.1021/jo301534b | J. Org. Chem. 2012, 77, 9044−9052

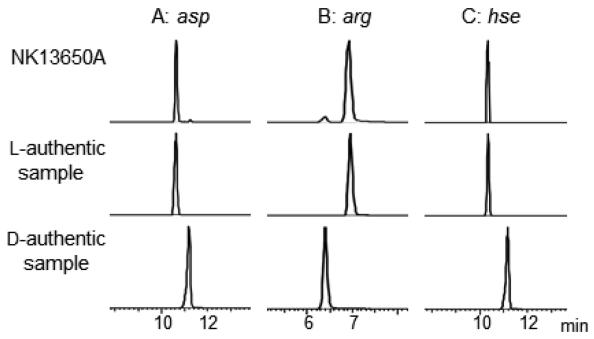

Figure 3. HPLC-HRESI-FTMS analyses of DLA derivatives. Upper line: derivatives of hydrolyzed NK13650A mixture. Middle line: derivatives of L-amino acids. Lower line: derivatives of D-amino acids. (A) Extracted ion chromatogram at m/z 428.1418 ± 0.004 for aspartic acid. (B) Extracted ion chromatogram at m/z 469.2159 ± 0.004 for arginine. (C) Extracted ion chromatogram at m/z 414.1625 ± 0.004 for homoserine.

caused by a different substituent group at *cit*1- and *cit*5-amides in citrate, to determine the stereochemistry a method requiring decomposition, such as the advanced Marfey's method, was not applicable. We used a new method based on NK13650 biosynthesis to elucidate the absolute structure. Citrate-containing peptide-like compounds are biosynthesized by the ordered constitution of two amides at the 1 and 5 positions in citrate.[35−37] The stereochemistries are accurately controlled during amide bond formation. Therefore, if the citrate, correctly labeled in the *pro-S* or *pro-R* carbon by a stable isotope ^{13}C, could be incorporated into NK13650A, the stereochemistry could be readily uncovered by ^{13}C NMR. However, obtaining such labeled citrate was not facile. Citrate is biosynthesized from acetyl-CoA and oxaloacetic acid by citrate synthase under strict stereochemical control, and the carboxylic acid of acetyl-CoA is arranged as the *pro-S* carboxylic acid of citrate in fungi and other major organisms, except for certain anaerobic bacteria.[38] Accordingly, it is assumed that feeding labeled acetyl-CoA or its biosynthetic precursor is equivalent to feeding labeled citrate (Scheme 1). First, feeding [1-^{13}C]acetate, which could be converted to acetyl-CoA by acetyl-CoA synthetase, was accomplished. ^{13}C-Labeled material was fed to the culture 8 days after inoculation when NK13650 production started. Unfortunately, the resulting NK13650A did not show incorporation of ^{13}C (Supporting Information). Then, [2-^{13}C]-pyruvate was used for the next feeding experiment, which is another approach to acetyl-CoA formation by the pyruvate dehydrogenase complex. In the ^{13}C NMR spectrum of the resulting NK13650A, the intensity of the signal at the *cit*1-amide carbon was slightly enhanced (Supporting Information). However, this result lacked clarity, and additional proof was needed. Subsequently, we performed a feeding experiment using [2,3-$^{13}C_2$]pyruvate. More definitive identification by ^{13}C NMR was expected because of $^1J_{C-C}$ coupling by which the peak for incorporation could be observed as an independent doublet signal. According to the method of our previous experiment, labeled NK13650A could be obtained using [2,3-$^{13}C_2$]pyruvate. The ^{13}C NMR spectrum of the resulting compound showed a doublet signal at the *cit*1-amide carbon (δ_C 169.5, $^1J_{C-C}$ = 50.6 Hz), whereas a weaker doublet peak was observed at *cit*5-amide (δ_C 169.7, $^1J_{C-C}$ = 50.6 Hz). The ratio of intensity of each signal was estimated to be 5:2 (Figure 4). This weak incorporation was believed to be caused by

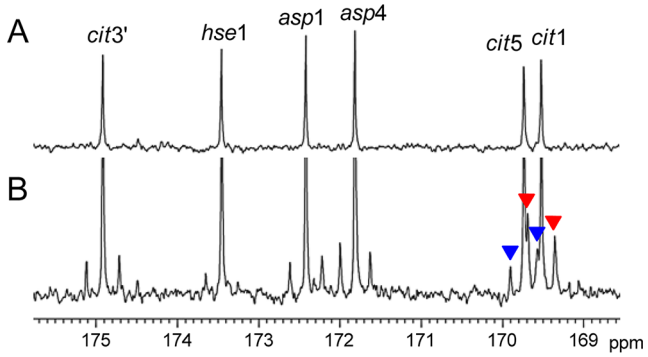

Figure 4. ^{13}C NMR spectra (150 MHz, in 0.5% TFA/DMSO-d_6) to estimate the incorporation of ^{13}C-labeled carbon atoms. (A) Spectrum for nonfeeding. (B) Spectrum for feeding [2,3-$^{13}C_2$]pyruvate. The doublet signal resulting from incorporation at *cit*1 is shown as a red triangle and at *cit*5 as a blue triangle.

carrying over the circuit of the citric acid cycle (Scheme 1). Because the rate of incorporation at cit5 was comparable to that at *cit*3′ (δ_C 174.9, $^1J_{C-C}$ = 51.3 Hz), the weak incorporation at *cit*5 could be ignored. Consequently, the last chiral center in

Scheme 1. Pathway of ^{13}C Incorporation from Pyruvic Acid to NK13650A[a]

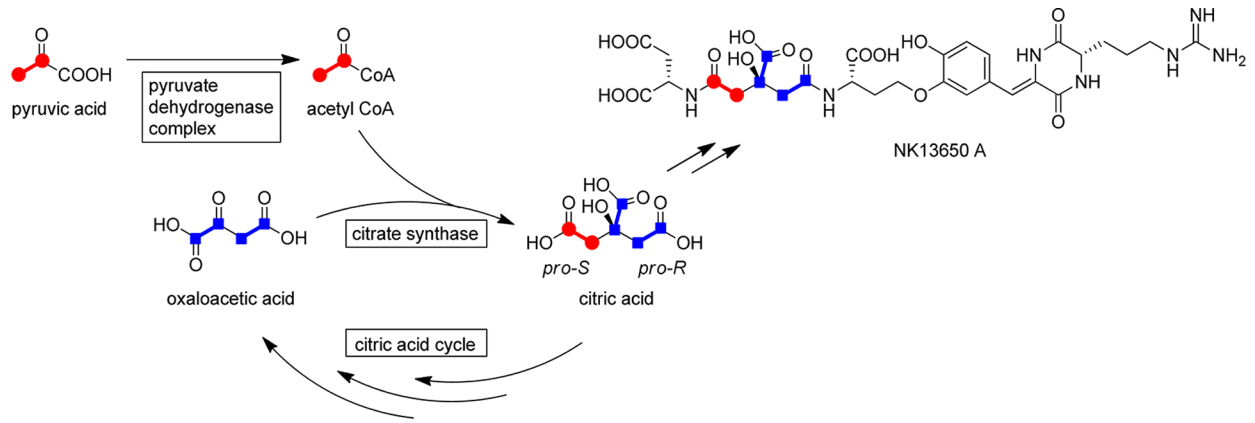

[a]Major incorporations without detours are shown as a red circle (●), and minor incorporations arising from circuits of the citric acid cycle are shown as a blue square (■).

dx.doi.org/10.1021/jo301534b | J. Org. Chem. 2012, 77, 9044−9052

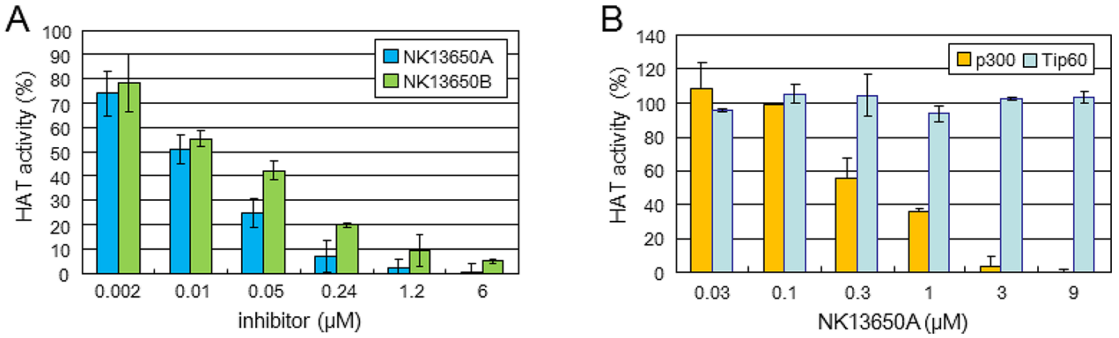

Figure 5. *In vitro* p300HAT inhibitory activities of NK13650s. (A) Relative HAT activities in the presence of NK13650A and NK13650B at several concentrations. (B) Selectivity of the inhibitory activities of NK13650A on p300 and Tip60 HAT. HAT activity is expressed as percent variation compared with that of the DMSO-treated sample. The graph summarizes the mean ± standard error.

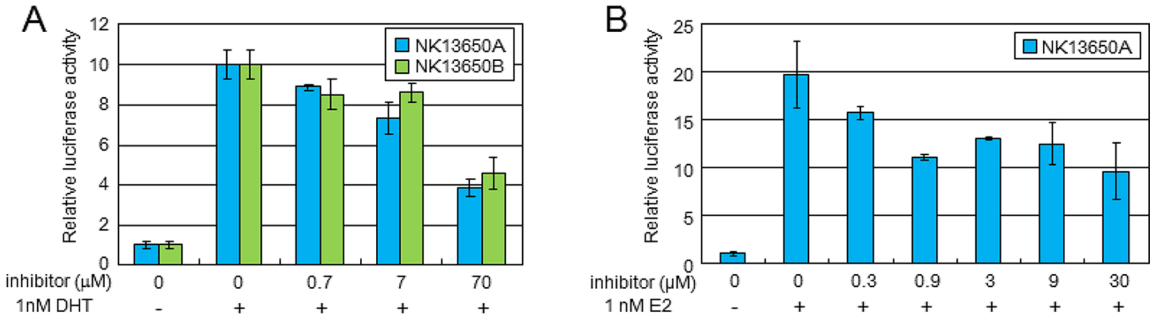

Figure 6. Suppression of hormone receptor-mediated transcriptional activation in cells. (A) Suppression of AR-mediated transcriptional activation by NK13650A and NK13650B. (B) Suppression of ER-mediated transcriptional activation by NK13650A. Relative luciferase activities were determined compared with those of the nontreated sample. The graph summarizes the mean ± standard error.

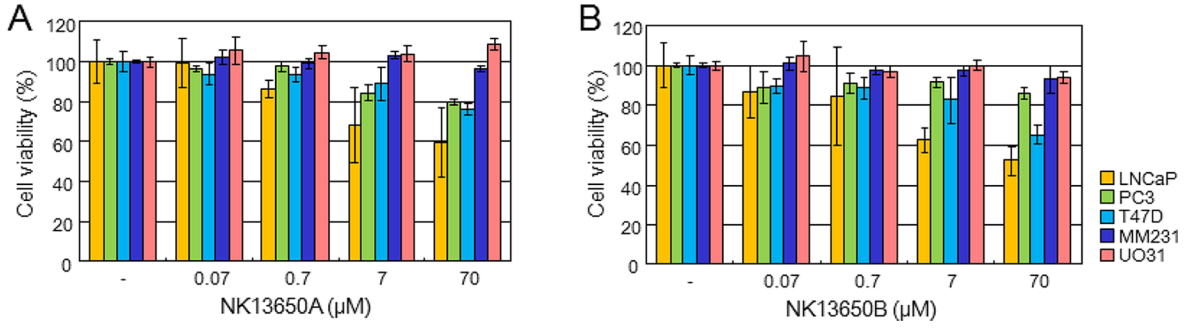

Figure 7. Treatment efficacies for the viabilities of several cancer cells. Selective cytotoxic activity of (A) NK13650A and (B) NK13650B. Relative activities were determined compared with those of the nontreated sample. The graph summarizes the mean ± standard error.

citrate was strongly sugested to have an *S* configuration (Figure 1).

Biological Activity of NK13650s. NK13650s showed HAT inhibitory activity against GST-p300C fusion protein in a dose-dependent manner at low concentration (Figure 5A). IC_{50} values of NK13650A and NK13650B were determined to be 11 and 22 nM, respectively. Lys-CoA, which is the substrate analogue of HAT and a well-known powerful HAT inhibitor,[28] showed an IC_{50} value of 3.2 nM (Supporting Information). Accordingly, NK13650s were regarded to be favorably comparable to previously reported HAT inhibitors. To further examine NK13650A specificity, Tip60, which has HAT activity and regulates AR function,[11] was used for comparison. The HAT activity of Tip60 showed no influence even in the presence of 9 μM NK13650A, whereas that of p300 could not be detected under the same condition (Figure 5B). This result suggests that NK13650s are strictly specific inhibitors of p300 HAT activity.

To ascertain whether NK13650s could suppress AR-mediated transcriptional activation in cells, we designed a system to detect the activity induced by dihydrotestosterone (DHT), a type of androgen, using genetically recombinant cells. Transient transfection of HEK-293 cells with an AR expression vector (pCMVAR-H) and a luciferase expression vector (pGL3MMTV-luc), which possesses the androgen response element (ARE) upstream of the reporter gene, was performed.[39] The luciferase activity of this construct showed sensitivity to DHT, which could be enhanced 10-fold in the presence of 1 nM DHT (Figure 6A). NK13650s clearly exhibited DHT inhibition in a dose-dependent manner (Figure 6A), whereas they could not influence constitutive luciferase expression (data not shown). These results suggest that NK13650s act via the AR-mediated transcriptional regulatory

dx.doi.org/10.1021/jo301534b | *J. Org. Chem.* 2012, 77, 9044−9052

machinery. Moreover, we examined the effect of NK13650A on estrogen (E2)-dependent estrogen receptor (ER)-α transcriptional activation using a similar methodology. This is because it is known that p300 HAT is also recruited to ER-α and ER-β in a ligand-dependent manner via interactions with the steroid receptor coactivator (SRC) family (i.e., SRC1, 2, and 3), which primarily functions as bridging factors to recruit other coregulators.[40] NK13650A suppressed luciferase expression by activating E2-dependent ER-α at >0.3 μM (Figure 6B).

The effect of NK13650s on the viability of cancer cells was investigated using the WST-8 assay in DHT-dependent LNCaP cell lines and DHT-independent PC-3 cell lines. Treatments with NK13650s increased the death of not only LNCaP cells but also PC-3 cells (Figure 7). These results suggest that NK13650s may overcome HRCP. Furthermore, NK13650s were also found to be cytotoxic to breast cancer cells, which require ER-mediated transcriptional activation. Estrogen-dependent T47-D cell growth was abolished by these p300 inhibitors, but estrogen-independent MDA-MB-231 cell growth was not affected. Moreover, these inhibitors did not decrease the viability of hormone-independent renal carcinoma UO31 cells.

DISCUSSION

NK13650A and NK13650B, which showed distinct p300 HAT inhibitory activities, were isolated as secondary metabolites produced by *Penicillium* species. Several HAT inhibitors (e.g., garcinol,[22] anacardic acid,[23] curcumin,[24] and triptolide[41]) have been reported, including several synthetic analogues,[26−30] but the structures of NK13650s are completely different from those of the other reported inhibitors. NK13650s have peptide-like structures containing citric acid, and the structures are commonly found in mycobacterial ferric iron chelators known as "siderophores",[35] examples of which include aerobactin of *Enterobacteriaceae*,[42] staphyloferrins of *Staphylococcus*,[43,44] and desferrioxamine E of *Actinobacteria*.[45] However, except for iron chelators, it has never been reported that compounds comprising citrate-containing peptide skeletons show particular bioactivities such as enzyme inhibition. Because of these structural characteristics, NK13650s presumably act as substrate histone mimics inhibiting HAT. Similar to HATs, many enzymes that modify proteins after translation have important roles in vital activities, such as protein kinases, methyltransferases, or acetyl transferases. The results of the present study suggest that citrate-containing peptide structures could be new scaffolds for such enzyme inhibitors. This result strongly indicates that microbial metabolites are attractive as drugs.

If citric acid has different substituents at C-1 and C-5 carboxyl groups, the C-3 quaternary carbon becomes a chiral center. Although citrate chiral centers were found in several citrate siderophores, only a few authors have determined the absolute configuration. To determine the stereochemistry at the citrate C-3 quaternary carbon of vibrioferrin, Takeuchi et al. performed total synthesis of both stereoisomers and compared their bioactivities.[46] In cases of staphyloferrins and rhizoferrins, these chiralities were revealed with circular dichroism (CD) spectra.[47−49] More recently, the stereochemistry of achromobactin was estimated by the enantioselectivity of AcsD, which catalyzes the first condensation of citric acid, using purified enzymes and enantiospecific ^{13}C-labeled citrate.[50] However, these methods lacked convenience and practicality, and it was believed that a novel, simple method was required. In the present study, we suggested that a new uncomplicated and applicable procedure could be developed, which could be readily accomplished by feeding ^{13}C-labeled acetate or pyruvate with subsequent ^{13}C NMR analyses. Although incorporations of labeled substrates were difficult in this case, this was probably possible because of the uniqueness of producing organisms or fermentation conditions. Acetic acid was incorporated into various metabolites via acetyl-CoA; therefore, easy determination of the citrate chiral center can be expected in other situations with the use of labeled acetic acid. To determine the stereochemistry completely, an additional certification, independent of biosynthetic origin, is maybe desired; however, we believe that a helpful method could be developed.

The biosynthesis of citrate siderophores has been well studied. It has been illustrated that first amine parts are biosynthesized, and eventually, the compound is produced after two amide formations at C-1 and C-5 carboxylic acids in citrate. In case of petrobactin in *Bacillus anthracis*, amide formations are catalyzed by two enzymes (called siderophore synthetases): AsbA for the first reaction and AsbB for the second one. AsbA mutants produce small quantities of petrobactin, whereas AsbB mutants produce only monosubstituted citrate intermediates. Therefore, AbsB is responsible for the second condensation and is expected to have weak substrate specificity. Schmelz et al. recently revealed the strict substrate specificity of AcsD, a siderophore synthetase that catalyzes first acyl transfer in achromobactin biosynthesis. According to their studies, AcsD catalyzed precisely the first condensation reaction of L-serine and C-5 *pro-R* carboxylic acid of citric acid. We investigated NK13650 biosynthesis. The first desymmetric condensation occurred at the *cit*5-carboxylic acid of citrate with the *hse-dhdopa-arg* moiety producing NK13650B as an intermediate. The second amide formation occurred with the addition of aspartate at the *cit*1-carboxylic acid of NK13650B, resulting in NK13650A. NK13650B is expected to be the precursor of NK13650A; therefore, NK13650B was considered to have an identical steric configuration.

NK13650s showed HAT inhibitory activities under very dilute conditions. IC_{50} values of NK13650A and NK13650B were determined to be 11 and 22 nM, respectively. These values were almost the same as the IC_{50} value of Lys-CoA (3.2 nM), which is a synthetic substrate analogue and the first class of inhibitors of p300 HAT.[28] It is not of huge consequence that the naturally occurring inhibitors reported until now show such strong activity comparable with that of Lys-CoA, although one author reported an IC_{50} value for Lys-CoA (0.5 μM)[28] that was distinct from the present study because of the difference in reaction conditions; we used 0.6 μM acetyl-CoA compared with 10 μM in their study. However, in the experiment using transfected cells with a luciferase reporter gene to detect AR function, much higher concentrations of acetyl-CoA were required to show the inhibitory activities of NK13650s.

NK13650A showed strict p300 HAT selectivity. Other HAT inhibitors have relatively broad specificities. Curcumin and garcinol inhibit p300 and pCAF,[22,24] and additionally, anacardic acid inhibits Tip60 as well as p300 and pCAF.[51] Different from those compounds, NK13650A did not show inhibitory activity against Tip60 HAT, although an IC_{50} value of 11 nM was indicated against p300. It is interesting how this selectivity arose because HATs catalyze the same reaction. The mechanism underlying this recognition might be revealed by cocrystal structure analyses of p300 and NK13650A, and the result could contribute to the design of new p300 HAT inhibitors.

dx.doi.org/10.1021/jo301534b | J. Org. Chem. 2012, 77, 9044−9052

As expected, NK13650s are cytotoxic to not only androgen-dependent LNCaP cells but also androgen-independent PC-3 prostate cancer cells, whereas they did not affect the viability of hormone-independent UO31 renal carcinoma cells. These findings suggest that NK13650s act as p300 HAT inhibitors in each cell and could be regarded as potentially new lead compounds for the treatment of androgen-independent prostate cancer. Moreover, NK13650s are cytotoxic to estrogen-dependent T47-D human breast cancer cells. ER also requires p300 HAT activity to function,[40] which is presumably why they can stunt the growth of T47-D cells. In contrast, estrogen-independent MDA-MB-231 breast cancer cells were not sensitive to NK13650s, suggesting that p300 HAT activity is not essential for these cells. In all cases, a higher concentration than the one used in the enzyme assay in vitro as well as the experiment using transfected cells was required to show the efficacy of NK13650s. Such observations are believed to result from the poor cellular permeability of these compounds, which show gross hydrophilicity. An attempt to determine the cellular concentration of NK13650 failed. If the permeation properties of NK13650s were improved by derivatizations or by using cell permeable formulations, NK13650s could exert their activities under lower concentrations and be used in drug development.

■ CONCLUSION

In the present study, we sought specific inhibitors as potential antiprostate cancer agents from culture broths of microorganisms. We discovered two novel compounds from the metabolites of the *Penicillium* sp. NF13650: NK13650A and NK13650B. These compounds had citrate-containing peptides. During demonstration of the absolute configuration at the C-3 position of citrate, we developed a useful method involving feeding a biosynthetic precursor of citrate. This methodology using strict stereoselectivity could be a powerful tool for the structural studies of natural products.

NK13650s showed specific inhibitory capacity against p300 HAT activity and had cytotoxic effects on androgen-dependent and -independent prostate cancer cells; it had no inhibitory activity against cancer cells that do not require functions of nuclear receptor. However, the effective concentrations against these cancer cells were even higher, despite their effectiveness at low concentrations against the enzyme. This disadvantage may be overcome by chemical modification. The derivatives may become potential drug candidates for the treatment of prostate cancer.

■ EXPERIMENTAL SECTION

General. HR ESIFT-MS spectra were obtained on a ThermoFisher Scientific LTQ Orbitrap XL mass spectrometer (Boston, MA, USA). All NMR spectra data were acquired in 0.5% TFA/DMSO-d_6 solution at 25 °C, and chemical shifts (δ) are given in ppm referring to the signal center using the solvent peaks for reference (δ_H 2.49 and δ_C 39.7). To accurately estimate incorporations of ^{13}C label, ^{13}C NMR measurements were performed under a high-resolution condition (0.722 Hz).

Cell Lines. Human embryonic kidney (HEK-293) cell line, human breast carcinoma (T47D, MDA-MB-231) cell lines, and human prostate carcinoma (LNCaP clone FGC, PC-3) were obtained from the American Type Culture Collection. Human renal carcinoma (UO-31) cells were obtained from the National Cancer Institute.

Cell Cultures. Established cell lines were maintained in RPMI 1640 media supplemented with 10% fetal bovine serum, with the exception of LNCaP cells, which were cultured in GIT medium. All cells were incubated at 37 °C in a humidified atmosphere with 5% CO_2.

Plasmids. The DNA sequence of the human p300 C-terminal domain (amino acid residues 1195−1673) was designed as an insert and subcloned into a pBlueScript II KS+ plasmid. After transformation of the plasmid in DH5α competent cells, the gene sequence was subcloned into the *Sal*I and *Not*I restriction sites of the pGEX-4T-1 expression vector. The DNA sequence of human Tip60 was designed as reported by Yamamoto and Horikoshi[52] and subcloned in the same manner. Preparations of the firefly luciferase reporter plasmid (pGL3MMTV), which contains ARE, and the full-length human AR expression plasmid (pCMVAR-H) were reported previously.[39]

Protein Expression. The pGEX 4T-1-p300C fusion and Tip60 vector were transformed into BL21(DE3)pLysS competent *Escherichia coli*. Production of the desired GST-p300C fusion product was verified by SDS-PAGE and confirmed by sequencing. Bacteria were harvested and resuspended in lysis buffer (PBS(−), 5 mM DTT, 1 mM PMSF, 0.1 mg/mL lysozyme, and 1% Triton X-100 at pH 7.4). A protease inhibitor cocktail was added at 10 μL/mL of resuspended pellet. The pellets were lysed by sonication and centrifuged at 14,000 rpm for 30 min at 4 °C. Fusion proteins were collected from the bacterial supernatant and purified by affinity chromatography using GSTrap FF prepared according to the manufacturer's instructions. The packed column was washed five times with PBS. An elution was run using 10 mM reduced glutathione in 50 mM Tris at pH 8.0. Collected fractions were assayed by SDS-PAGE; pooled fractions were treated with the protease inhibitor cocktail and dialyzed three times against PBS(−). Purity was confirmed by FPLC and SDS-PAGE.

HAT Activity Inhibition Assays. The assay used in our laboratory is based on that described previously.[31] GST-p300C fusion recombinant protein (18.5 nM) or GST-Tip60 recombinant protein (17 nM) was incubated in HAT buffer (50 mM Tris-HCl pH 7.5, 10% glycerol, 0.5 mM EDTA, 0.1% BSA, 1 mM DTT, and 0.1 mM PMSF) with 50 μg/mL of lysine-rich histone fraction, type IIIS and 0.6 μM acetyl-CoA containing 50 μCi/mL [^{3}H]-acetyl-CoA in the presence of NK13650s at selected concentrations. Assays were performed in 1.5 mL plastic tubes at 30 °C, and the reaction volumes were 30 μL. After 30 min, the reactions were stopped by adding 70 μL of wash buffer (50 mM sodium carbonate, pH 9.2) and followed by spotting onto Hybond N$^+$ membranes. The membranes were washed three times with 200 μL of wash buffer. Then, 20 μL of scintillation fluid was added to allow the DPM reading in a microplate scintillation counter. DPM of enzyme samples was compared with that of the negative control. Data are expressed as percentages.

Fermentation. For NK13650 production, the producing strain *Penicillium* sp. NF13650 was cultivated in 500-mL baffled flasks containing 50 mL of production medium (sucrose 8%, soybean meal 0.5%, gluten meal 1.5%, yeast extract 0.2%, KH_2PO_4 0.05%, KCl 0.1%, $MgSO_4$ 0.05%, $CoCl_2$ 0.0001%, $CuSO_4$ 0.00064%, $FeSO_4$ 0.00011%, $MnCl_2$ 0.00079%, and $ZnSO_4$ 0.00015%). After the culture was shaken (200 rpm) for 2 days at 25 °C, materials for NK13650 biosynthesis (L-homoserine 0.5%, sodium L-aspartate 0.5%, L-tyrosine 0.5%, L-arginine 0.5%, and citric acid 0.5%) were added to each flask. An additional culture was accomplished under the static condition for 14 days at 25 °C.

Purification of NK13650s. The fermentation broth (4 L) was combined and centrifuged. After the pH was adjusted to 2 with HCl, the obtained supernatant was passed through a MCI gel CHP20P column to adsorb NK13650. The column was eluted with 30% aqueous methanol, and appropriate fractions were combined and concentrated under reduced pressure. The resulting mixture was subjected to Sephadex G10 column chromatography using water as the elution solvent to separate NK13650A and NK13650B. The fractions containing NK13650A and NK13650B were gathered separately and concentrated under reduced pressure. Each residue obtained was further purified by reverse phase HPLC using a Capcell Pak UG 120 (20 mm × 250 mm, 5 μm) column. The column was eluted with 0.1% formic acid in 18% aqueous methanol to obtain pure NK13650A (18 mg) and NK13650B (3 mg). NK13650A: white powder; $[\alpha]^{22}_D$ = −157 (*c* 0.15, H_2O); IR (KBr) ν_{max} 3407, 1720, 1668, 1635,1550,

dx.doi.org/10.1021/jo301534b | J. Org. Chem. 2012, 77, 9044−9052

1519, 1427, 1390,1342, 1276, 1238, 1184 cm^{-1}; UV (H_2O) λ_{max} (log ε) 222 (sh, 4.18), 236 (sh, 4.14), 309 (sh, 4.15), 325 (4.22) nm; HR ESI FTMS m/z 724.2410 $[M + H]^+$ (calcd for $C_{29}H_{38}N_7O_{15}$, 724.2420). NK13650B: white powder; $[\alpha]^{40}_D = -111$ (c 0.1, AcOH); IR (KBr) ν_{max} 3415, 1668, 1635, 1519,1475, 1427, 1394, 1344,1278, 1182, 1130, 1043 cm^{-1}; UV (H_2O) λ_{max} (log ε) 220 (sh, 4.22), 238 (sh, 4.13), 309 (sh, 4.07), 325 (4.13) nm; HR ESI FTMS m/z 609.2154 $[M + H]^+$ (calcd for $C_{25}H_{33}N_6O_{12}$, 609.2151).

Advanced Marfey's Method. A solution of NK13650 (0.1 mg) in 1 mL of 6 M HCl was sealed in a tube and heated at 110 °C for 20 h. The reaction mixture was concentrated under reduced pressure to dryness, and the resulting residue was dissolved in 50 μL of water. Subsequently, 20 μL of 1 M $NaHCO_3$ and 100 μL of 1% L-FDLA were added to the solution. The reaction mixture was incubated at 37 °C for 1 h. After quenching by the addition of 20 μL of 1 M HCl, 10 μL of the resulting solution was diluted with 90 μL of acetonitrile to prepare the sample for subsequent LC–MS analyses. Authentic samples (L-FDLA-requiring derivatives of both stereoisomers of aspartate, arginine, and homoserine) were prepared according to the same procedure. All samples were analyzed by HPLC–MS using a Capcell Pak C18 UG 120 (2.0 mm ×150 mm) column by linear gradient elution with 0.01% trifluoroacetic acid (TFA) in acetonitrile/0.01% TFA in water (20:80 to 80:20) in 30 min at a flow rate of 200 μL/min. We monitored the protonated molecules (m/z 428.1418 for aspartic acid, 469.2159 for arginine, and 414.1625 for homoserine) by HR ESIFT-MS.

Feeding Experiment. Fermentation was accomplished by a procedure similar to the above-mentioned one. After the culture (1.5 L) was shaken for 2 days, biosynthetic materials except for citric acid were added to each flask. Six days later, 1 mL of filter-sterilized sodium [2,3-$^{13}C_2$]pyruvate solution (96.8 mg/mL) was added to each flask, and fermentation was continued for 6 days. Purification was accomplished according to the above-mentioned procedure; 7.3 mg of labeled NK13650A was obtained.

Luciferase Assays. HEK-293 cells were plated in 96-well dishes at 2×10^4 cells/mL. After attachment, the cells were transfected using 0.5 μL/well lipofectamine 2000 with 20 ng/well pGL3-MMTV, 1 ng/well pRL (Renilla luciferase)-CMV as an internal control, and a 20-ng/well expression vector for AR. Four hours after transfection, 0.5 mL of DMEM containing 10% dextran/charcoal-treated FBS, with or without 1 nM dihydrotestosterone (DHT), and NK13650s at the indicated concentrations was added; 48 h after transfection, the cells were lysed in lysis buffer for the luciferase assay. The reporter gene activities were determined using Envision and are expressed as values normalized by pRL-induced activities, i.e., (firefly luciferase activity)/(Renilla luciferase activity). All experiments were repeated at least twice. Data are expressed as mean ± SD.

Cell Growth Inhibition Assay. Each cell line was plated in 96-well dishes at 2,000 cells/well (10,000 cells/mL). After attachment, 0.2 mL of DMEM containing 10% dextran/charcoal-treated FBS, with or without 1 nM DHT, and NK13650s at the indicated concentrations was added. All samples contained a final concentration of ≤0.1% DMSO. Vehicle samples were treated with cell culture media containing 0.1% DMSO. The cells were incubated with compounds for 6 days, followed by the addition of 20 μL WST-8 reagent to each well. The dishes were incubated at 37 °C and 5% CO_2 for 4 h before reading the absorbance at 450 nm (650 nm as a reference) on a Benchmark plus microplate reader.

■ ASSOCIATED CONTENT

Ⓢ Supporting Information

^1H and ^{13}C NMR spectra for NK13650s. Structural analyses for NK13650B. Results of feeding experiments of [1-^{13}C]acetate and [2-^{13}C]pyruvate. In vitro p300HAT inhibitory activities of Lys-CoA. This material is available free of charge via the Internet at http://pubs.acs.org.

■ AUTHOR INFORMATION

Corresponding Author

*E-mail: tohyamas@bikaken.or.jp; arihiro.tomura@nipponkayaku.co.jp.

Notes

The authors declare no competing financial interest.

■ REFERENCES

(1) Glozak, M. A.; Sengupta, N.; Zhang, X. H.; Seto, E. *Gene* **2005**, *363*, 15–23.
(2) Culig, Z.; Klocker, H.; Bartsch, G.; Steiner, H.; Hobisch, A. *J. Urol.* **2003**, *170*, 1363–1369.
(3) Agarwal, N.; Hutson, T. E.; Vogelzang, N. J.; Sonpavde, G. *Future Oncol.* **2010**, *6*, 665–679.
(4) Taplin, M. E. *Nat. Clin. Pract. Oncol.* **2007**, *4*, 236–244.
(5) Gleave, M. E.; Small, E. J. *Report to the Nation on Prostate Cancer 2004; Androgen Deprivation Therapy for Prostate Cancer*; Prostate Cancer Foundation: Santa Monica, CA, 2004; pp 27–36.
(6) Faus, H.; Haendler, B. *J. Cell Biochem.* **2008**, *104*, 511–524.
(7) Kaikkonen, S.; Jaaskelainen, T.; Karvonen, U.; Rytinki, M. M.; Makkonen, H.; Gioeli, D.; Paschal, B. M.; Palvimo, J. J. *Mol. Endocrinol.* **2009**, *23*, 292–307.
(8) Lin, H. K.; Wang, L.; Hu, Y. C.; Altuwaijri, S.; Chang, C. *EMBO J.* **2002**, *21*, 4037–4048.
(9) Ogryzko, V. V.; Schiltz, R. L.; Russanova, V.; Howard, B. H.; Nakatani, Y. *Cell* **1996**, *87*, 953–959.
(10) Bannister, A. J.; Kouzarides, T. *Nature* **1996**, *384*, 641–643.
(11) Halkidou, K.; Gnanapragasam, V. J.; Mehta, P. B.; Logan, I. R.; Brady, M. E.; Cook, S.; Leung, H. Y.; Neal, D. E.; Robson, C. N. *Oncogene* **2003**, *22*, 2466–2477.
(12) Fu, M.; Wang, C.; Reutens, A. T.; Wang, J.; Angeletti, R. H.; Siconolfi-Baez, L.; Ogryzko, V.; Avantaggiati, M. L.; Pestell, R. G. *J. Biol. Chem.* **2000**, *275*, 20853–20860.
(13) Fu, M.; Wang, C.; Wang, J.; Zhang, X.; Sakamaki, T.; Yeung, Y. G.; Chang, C.; Hopp, T.; Fuqua, S. A.; Jaffray, E.; Hay, R. T.; Palvimo, J. J.; Janne, O. A.; Pestell, R. G. *Mol. Cell. Biol.* **2002**, *22*, 3373–3375.
(14) Culig, Z.; Comuzzi, B.; Steiner, H.; Bartsch, G.; Hobisch, A. *J. Steroid Biochem. Mol. Biol.* **2004**, *92*, 265–271.
(15) Debes, J. D.; Sebo, T. J.; Lohse, C. M.; Murphy, L. M.; Haugen, D. A.; Tindall, D. J. *Cancer Res.* **2003**, *63*, 7638–7640.
(16) Debes, J. D.; Schmidt, L. J.; Huang, H.; Tindall, D. J. *Cancer Res.* **2002**, *62*, 5632–5636.
(17) Dekker, F. J.; Haisma, H. J. *Drug Discovery Today* **2009**, *14*, 942–948.
(18) Roelfsema, J. H.; Peters, D. J. *Expert Rev. Mol. Med.* **2007**, *9*, 1–16.
(19) Giles, R. H.; Peters, D. J.; Breuning, M. H. *Trends Genet.* **1998**, *14*, 178–183.
(20) FDA. *J. Natl. Cancer Inst.* **2010**, *102*, 219.
(21) Mann, B. S.; Johnson, J. R.; Cohen, M. H.; Justice, R.; Pazdur, R. *Oncology* **2007**, *12*, 1247–1252.
(22) Balasubramanyam, K.; Altaf, M.; Varier, R. A.; Swaminathan, V.; Ravindran, A.; Sadhale, P. P.; Kundu, T. K. *J. Biol. Chem.* **2004**, *279*, 33716–33726.
(23) Balasubramanyam, K.; Swaminathan, V.; Ranganathan, A.; Kundu, T. K. *J. Biol. Chem.* **2003**, *278*, 19134–19140.
(24) Balasubramanyam, K.; Varier, R. A.; Altaf, M.; Swaminathan, V.; Siddappa, N. B.; Ranga, U.; Kundu, T. K. *J. Biol. Chem.* **2004**, *279*, 51163–51171.
(25) Ravindra, K. C.; Selvi, B. R.; Arif, M.; Reddy, B. A. A.; Thanuja, G. R.; Agrawal, S.; Pradhan, S. K.; Nagashayana, N.; Dasgupta, D.; Kundu, T. K. *J. Biol. Chem.* **2009**, *284*, 24453–24464.
(26) Costi, R.; Di Santo, R.; Artico, M.; Miele, G.; Valentini, P.; Novellino, E.; Cereseto, A. *J. Med. Chem.* **2007**, *50*, 1973–1977.
(27) Stimson, L.; Rowlands, M. G.; Newbatt, Y. M.; Smith, N. F.; Raynaud, F. I.; Rogers, P.; Bavetsias, V.; Gorsuch, S.; Jarman, M.; Bannister, A.; Kouzarides, T.; McDonald, E.; Workman, P.; Aherne, G. W. *Mol. Cancer Ther.* **2005**, *4*, 1521–1532.

(28) Lau, O. D.; Kundu, T. K.; Soccio, R. E.; Ait-Si-Ali, S.; Khalil, E. M.; Vassilev, A.; Wolffe, A. P.; Nakatani, Y.; Roeder, R. G.; Cole, P. A. *Mol. Cell* **2000**, *5*, 589−595.
(29) Kwie, F. H.; Briet, M.; Soupaya, D.; Hoffmann, P.; Maturano, M.; Rodriguez, F.; Blonski, C.; Lherbet, C.; Baudoin-Dehoux, C. *Chem. Biol. Drug Des.* **2011**, *77*, 86−92.
(30) Liu, X.; Wang, L.; Zhao, K.; Thompson, P. R.; Hwang, Y.; Marmorstein, R.; Cole, P. A. *Nature* **2008**, *451*, 846−850.
(31) Wynne Aherne, G.; Rowlands, M. G.; Stimson, L.; Workman, P. *Methods* **2002**, *26*, 245−253.
(32) Miller, T. W.; Chaiet, L.; Arison, B.; Walker, R. W.; Trenner, N. R.; Wolf, F. J. *Antimicrob. Agents Chemother.* **1963**, *161*, 58−62.
(33) Fujii, K.; Ikai, Y.; Mayumi, T.; Oka, H.; Suzuki, M.; Harada, K. *Anal. Chem.* **1997**, *69*, 3346−3352.
(34) Fujii, K.; Ikai, Y.; Oka, H.; Suzuki, M.; Harada, K. *Anal. Chem.* **1997**, *69*, 5146−5151.
(35) Challis, G. *ChemBioChem* **2005**, *6*, 601−611.
(36) Lee, J. Y.; Janes, B. K.; Passalacqua, K. D.; Pfleger, B. F.; Bergman, N. H.; Liu, H.; Hakansson, K.; Somu, R. V.; Aldrich, C. C.; Cendrowski, S.; Hanna, P. C.; Sherman, D. H. *J. Bacteriol.* **2007**, *189*, 1698−1710.
(37) Berti, A. D.; Thomas, M. G. *J. Bacteriol.* **2009**, *191*, 4594−4604.
(38) Marco-Urrea, E.; Paul, S.; Khodaverdi, V.; Seifert, J.; von Bergen, M.; Kretzschmar, U.; Adrian, L. *J. Bacteriol.* **2011**, *193*, 5171−5178.
(39) Tomura, A.; Goto, K.; Morinaga, H.; Nomura, M.; Okabe, T.; Yanase, T.; Takayanagi, R.; Nawata, H. *J. Biol. Chem.* **2001**, *276*, 28395−28401.
(40) McKenna, N. J.; Lanz, R. B.; O'Malley, B. W. *Endocr. Rev.* **1999**, *20*, 321−344.
(41) Park, B.; Sung, B.; Yadav, V. R.; Chaturvedi, M. M.; Aggarwal, B. B. *Biochem. Pharmacol.* **2011**, *82*, 1134−1144.
(42) Gibson, F.; Magrath, D. I. *Biochim. Biophys. Acta* **1969**, *192*, 175−184.
(43) Konetschnyrapp, S.; Jung, G.; Meiwes, J.; Zahner, H. *Eur. J. Biochem.* **1990**, *191*, 65−74.
(44) Drechsel, H.; Freund, S.; Nicholson, G.; Haag, H.; Jung, O.; Zahner, H.; Jung, G. *Biometals* **1993**, *6*, 185−192.
(45) Hossain, M. B.; Vanderhelm, D.; Poling, M. *Acta Crystallogr., Sect. B* **1983**, *39*, 258−263.
(46) Takeuchi, Y.; Nagao, Y.; Toma, K.; Yoshikawa, Y.; Akiyama, T.; Nishioka, H.; Abe, H.; Harayama, T.; Yamamoto, S. *Chem. Pharm. Bull.* **1999**, *47*, 1284−1287.
(47) Drechsel, H.; Jung, G.; Winkelmann, G. *Biometals* **1992**, *5*, 141−148.
(48) Munzinger, M.; Taraz, K.; Budzikiewicz, H. *Z. Naturforsch. C* **1999**, *54*, 867−875.
(49) Drechsel, H.; Winkelmann, G. I. *Biometals* **2005**, *18*, 75−81.
(50) Schmelz, S.; Kadi, N.; McMahon, S. A.; Song, L.; Oves-Costales, D.; Oke, M.; Liu, H.; Johnson, K. A.; Carter, L. G.; Botting, C. H.; White, M. F.; Challis, G. L.; Naismith, J. H. *Nat. Chem. Biol.* **2009**, *5*, 174−182.
(51) Sung, B.; Pandey, M. K.; Ahn, K. S.; Yi, T.; Chaturvedi, M. M.; Liu, M.; Aggarwal, B. B. *Blood* **2008**, *111*, 4880−4891.
(52) Yamamoto, T.; Horikoshi, M. *J. Biol. Chem.* **1997**, *272*, 30595−30598.

■ NOTE ADDED AFTER ASAP PUBLICATION

The alignment of the *dhdopa* section in Table 1 was incorrect in the version published ASAP September 27, 2012; the correct version reposted October 8, 2012.